Air Substrate Slot Array Based on Channelized Coplanar Waveguide

Le Chang, *Student Member, IEEE*, Zhijun Zhang, *Fellow, IEEE*, Yue Li, *Member, IEEE*, and Magdy F. Iskander, *Fellow, IEEE*

***Abstract*—A new structure of planar air substrate slot antenna array based on air-filled channelized coplanar waveguide is proposed. By blocking the channelized coplanar waveguide alternatively and periodically, the subslot array is constructed. By connecting eight subslot arrays in a mirrored way, the proposed planar slot antenna array is built. A line source is used as the feed network, and the center-fed approach is adopted to suppress beam tilt. Because of the layout of the proposed slot array and the feed network, the shorting walls at the interconnecting planes of the neighboring subarrays can be removed, resulting in a compact structure. A prototype with a gain up to 22.75 dBi and an impedance bandwidth of 6.4% is fabricated to demonstrate the design strategy.**

***Index Terms*—Air substrate antenna, channelized coplanar waveguide, slot array antenna.**

I. Introduction

DIELECTRIC loss becomes a severe issue in high frequency usage, especially when the antenna array dimension is large. Many published works have been studied on how to remove dielectric substrate to improve antenna performance [1]–[4]. One is by removing a portion of the substrate using backside etching process to improve bandwidth and efficiency [1]. The air-layer addition technique in low temperature cofired ceramic (LTCC) fabrication was adopted to remove the dielectrics of the parallel-plate slot arrays [2]–[4]. Using removable dummy plates or sublimable dummy materials, air regions were inserted in the radiating/feeding part, resulting in enhanced gain and bandwidth performance.

Air substrate antennas can avoid the adverse effects caused by dielectrics. Air substrate cavity-cascaded antennas based on microstrip line have been proposed by the authors [5]–[7]. In this letter, a new structure of planar air substrate slot antenna array based on air-filled channelized coplanar waveguide (ACCPW) is proposed [8]. The subslot array is constructed by alternatively loading the ACCPW with blocking stubs every half-wavelength: In this way, the fringing fields along one direction are suppressed, while fields along the other direction are left within the naturally generated slots, forming a large in-phase radiating aperture. Moreover, the slot number can be easily expanded to achieve a slightly higher gain. Eight subslot arrays are connected together with the neighboring subarrays mirrored with each other to constitute the final planar slot array. An eight-way power divider and eight coupling slots located at the array center are used as the feed network. Owing to the reverse excitation phase of the neighboring subarrays, the shorted walls that should be at the interconnecting planes can be removed, resulting in a compact antenna structure. The fabricated prototype shows a bandwidth of 6.4% and a peak gain of 22.75 dBi at K-band.

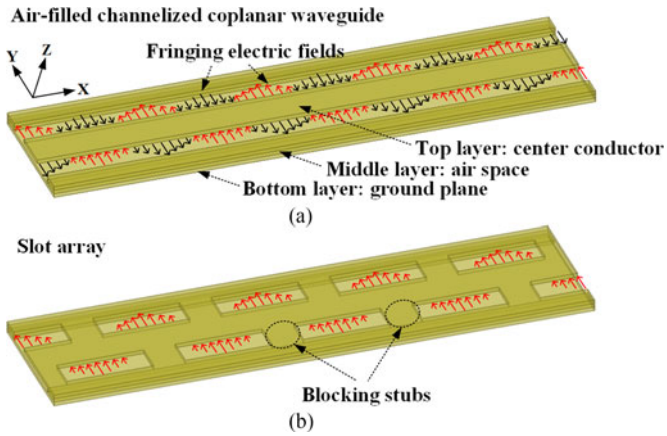

Fig. 1. Radiation principle. (a) Three-layer channelized coplanar waveguide and (b) slot array generated by alternatively loading periodical blocking stubs.

II. Radiation Principle

ACCPW consists of three layers as shown in Fig. 1(a), which is evolved from the CPW structure, and detailed description can be found in [8]. The air space in the middle layer reserves room for wave propagating. The electric fields on one side of the center conductor are out of phase with their counterparts on the other side. Thus, the wave is confined and propagating within the air space between the center conductor and the ground.

Based on periodicity, blocking stubs are loaded to the center conductor alternatively every half-wavelength for effective ra-

Manuscript received July 5, 2016; revised August 16, 2016; accepted September 23, 2016. Date of publication September 27, 2016; date of current version April 10, 2017. This work was supported in part by the National Basic Research Program of China under Contract 2013CB329002, in part by the National Natural Science Foundation of China under Contract 61525104 and Contract 61331003, and in part by the China Postdoctoral Science Foundation under Project 2015T80084.

L. Chang, Z. Zhang, and Y. Li are with the State Key Lab on Microwave and Communications, Tsinghua National Laboratory for Information Science and Technology, Tsinghua University, Beijing 100084, China (e-mail: changle4015@126.com; zjzh@tsinghua.edu.cn; lyee@tsinghua.edu.cn).

M. F. Iskander is with the Hawaii Center for Advanced Communications, University of Hawaii at Manoa, Honolulu, HI 96822 USA (e-mail: iskander@spectra.eng.hawaii.edu).

Color versions of one or more of the figures in this letter are available online at http://ieeexplore.ieee.org.

Digital Object Identifier 10.1109/LAWP.2016.2613965

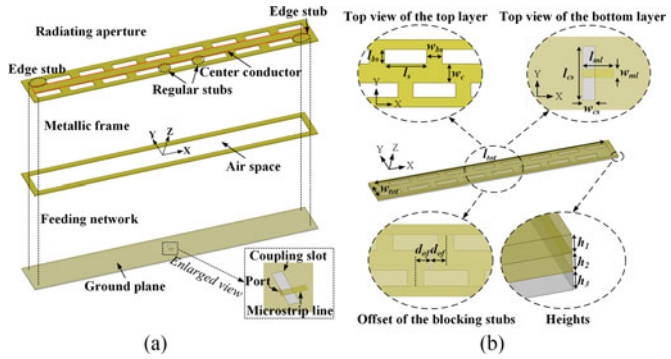

Fig. 2. (a) Geometry and (b) detailed parameters depicting the subslot array.

TABLE I
DETAILED DIMENSIONS OF THE SUBSLOT ARRAY (UNIT: mm)

Parameter	l_{tot}	w_{tot}	w_c	l_s	l_{bs}	w_{bs}	d_{of}
Value	123.5	12.5	4.9	11	3.8	4	3.75
Parameter	l_{cs}	w_{cs}	l_{ml}	w_{ml}	h_1	h_2	h_3
Value	4.5	1	2	0.7	0.5	0.5	0.51

diation as illustrated in Fig. 1(b). The fringing fields along the $-Y$-direction, denoted by the black arrow lines, are suppressed while fields along the $+Y$-direction, denoted by the light arrow lines, are left within these naturally generated slots. Finally, the field in each slot is with identical phase, forming an in-phase aperture. Thus, these blocking stubs turn the ACCPW into a slot array antenna. Moreover, it has scalable capability along the X-direction to achieve a slightly higher gain.

III. SUBSLOT ARRAY

Fig. 2 shows the K-band three-layer subslot array. The center conductor is loaded with 16 half-wavelength-spaced blocking stubs, forming 16 radiating slots. The middle layer is the metallic frame, which has two functions: First, it is used to support the top layer and reserves air space for wave propagating; second, it creates an electric-wall boundary to confine the wave. The bottom layer provides the feed network based on the Taconic TLX-8 substrate ($\varepsilon_r = 2.55$, $\tan\delta = 0.0019$). An enlarged view of the coupling slot and microstrip line is given in the inset: The microstrip line lying at the bottom crosses the center of the coupling slot, which lies in the center of the subarray. The alignment of the three layers is illustrated by the four dotted vertical lines. Detailed dimensions are shown in Fig. 2(b) and Table I. The antenna is designed using the software High Frequency Structure Simulator (HFSS) version 14.

The height of the air space (middle frame layer) is an important parameter influencing directivity. Three height values are analyzed to understand its effect. In each case, the lengths of the coupling slot and microstrip line are adjusted to achieve good impedance matching at 20 GHz. The magnitudes of the reflection coefficients and broadside directivities at 20 GHz under the three heights together with the matching-adjustment parameter values are listed in Table II. When the height increases from 0.5 to 1 mm, directivity decreases by 0.57 dB from 18.92 to 18.35 dBi. Further increasing to 1.5 mm causes a 2.84-dB gain drop. This is caused because the radiation ability of each

TABLE II
$|S_{11}|$ AND BROADSIDE DIRECTIVITY AT 20 GHz UNDER THREE HEIGHTS

h_2 /mm	0.5	1.0	1.5
(l_{cs}, l_{ml})/mm	(4.5, 2)	(5.6, 1)	(5.4, 0.55)
$\lvert S_{11}\rvert$/dB	–36.09	–30.88	–34.40
Directivity /dBi	18.92	18.35	15.51

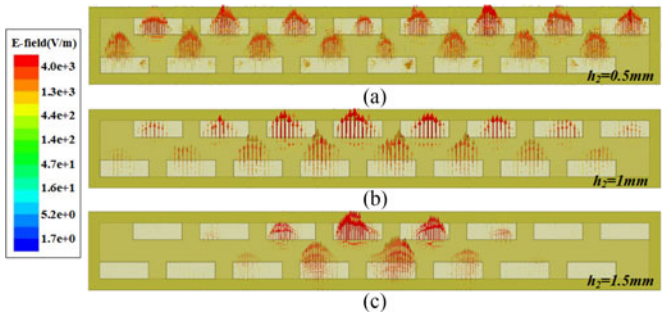

Fig. 3. Aperture vector electric field distributions at 20 GHz under the middle-layer heights of (a) $h_2 = 0.5$ mm, (b) $h_2 = 1.0$ mm, and (c) $h_2 = 1.5$ mm. (Fields are sampled in the surface of the radiating aperture.)

TABLE III
DIRECTIVITY AT 20 GHz VARYING WITH THE SLOT NUMBER

Slot number	4	6	8	10	12
Directivity/dBi	11.05	14.02	15.81	16.98	17.85
Slot number	14	16	18	20	22
Directivity/dBi	18.43	18.92	19.21	19.47	19.61

slot gets stronger with the increase of the height. The aperture vector electric field distributions are presented in Fig. 3: A half-period wave in each slot exists, and the aperture amplitude decreases from the center to two ends gradually. As the height reaches 1.5 mm, most of the energy is radiated out by several slots located near the center, and the outer slots exhibit a weaker excitation. This fact suggests that the array is operating in a travelling-wave mode, rather than a standing-wave mode. When the height decreases, the radiation ability of each slot becomes weak, so more energy will be transmitted to both sides, resulting in a more uniform aperture amplitude distribution. As seen, the aperture amplitude becomes more and more uniform as the height decreases from 1.5 to 0.5 mm. When the height is at 0.5 mm, clear antinodes and nodes are observed, indicating that the array is operating as a standing-wave mode. Lower height leads to a higher directivity. In this letter, gain is the priority consideration, so the height selected is 0.5 mm.

As discussed previously, this kind of antenna is scalable and can achieve a slightly higher gain. Broadside directivities at 20 GHz varying with the slot/stub number are given in Table III. Directivity increases as more stubs are loaded and the growth trend follows the logarithmic distribution. Considering the continuing slow growth rate, the stub number of 16 is a good compromise between size and directivity.

IV. PLANAR SLOT ANTENNA ARRAY

The geometry of the proposed planar slot antenna array is shown in Fig. 4. It is a three-layer structure as the subarray. The proposed planar array consists of eight columns of the subarrays

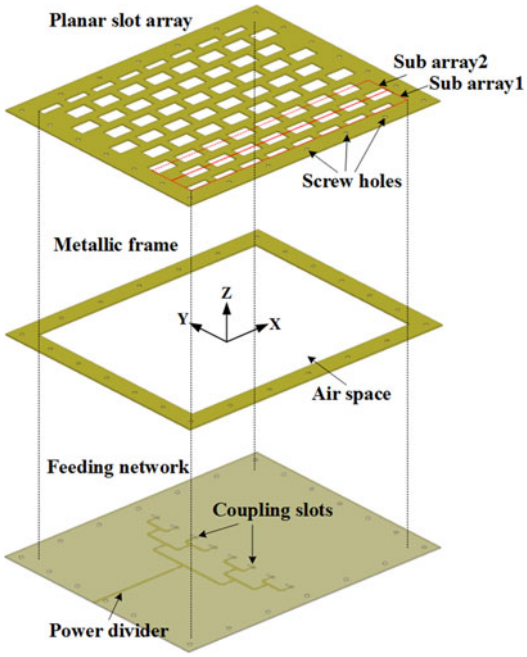

Fig. 4. Geometry of the proposed planar slot antenna array.

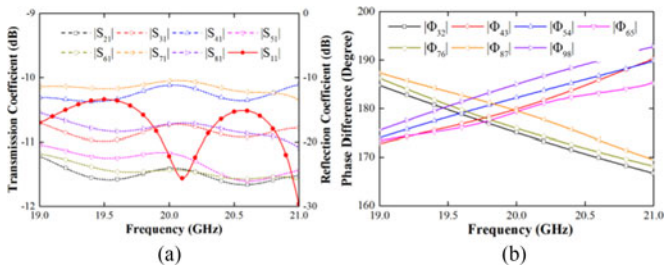

Fig. 5. (a) Magnitudes of the reflection and transmission coefficients and (b) transmission phase difference between the neighboring outputs of the eight-way power divider.

and the neighboring subarrays, such as subarrays 1 and 2 denoted by the dotted parallelograms, have mirror relations. These neighboring slots of the two adjacent subarrays are combined into bigger ones. The middle layer is a compact metallic frame just as that of the subarray, and the bottom is the feed network layer based on the same substrate. An eight-way power divider, whose output amplitudes are uniform and the adjacent outputs are phase-reversed, is used to excite the proposed array through eight coupling slots. Twenty-four screw holes with the same 2-mm diameter surrounding the antenna are used to assemble the three layers. Dimensions of the blocking stubs and coupling slots are the same as that of the subarray. The radiating aperture of the proposed array measures $123.5 \times 100\ \text{mm}^2$ ($8.23\lambda_0 \times 6.67\lambda_0$).

The power divider consists of three types of transmission lines, namely, the quarter-wavelength impedance transformers with characteristic impedances of 71 Ω and 50 Ω and the microstrip line with characteristic impedance of 50 Ω. The simulated performance is given in Fig. 5. At 20 GHz, the magnitude of the reflection coefficient is better than –20 dB, and the transmission coefficients fluctuate within 1.5 dB, ranging from –10.05 to –11.50 dB; the phase differences fluctuate around 180° with a phase error less than ±5°.

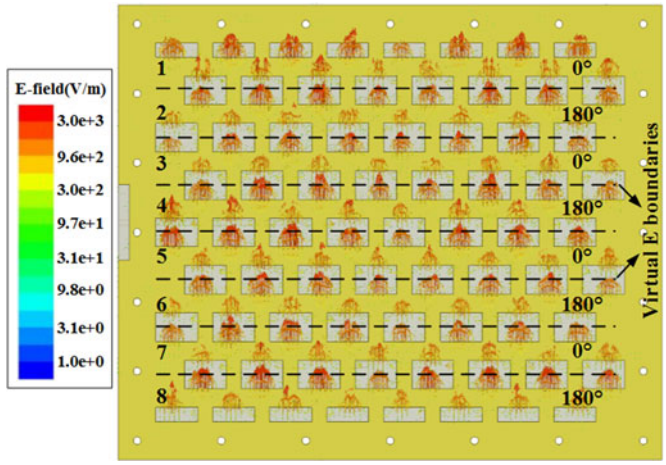

Fig. 6. Operation principle and vector electric field distribution at 20 GHz. (Field is sampled in the surface of the radiating aperture.)

The operation principle and vector electric field distribution are illustrated in Fig. 6. The excitation phases are reversed alternatively as marked in the figure. Thus, virtual electric-wall boundaries as denoted by the dashed lines are generated in the interconnecting planes between neighboring subarrays. In this way, the realistic shorted walls in these dashed-line positions can be omitted, resulting in a compact middle frame layer. The seven virtual electric-wall boundaries together with the two side edges of the metallic frame restrict the wave of each subarray resonate within its own respective space, without interfering with each other. On the other hand, the adjacent subarrays are mirrored with each other. Finally, as shown, the fields of all the 8×16 slots are with the identical phase, forming a large in-phase radiating aperture. In addition, the phase distribution can effectively suppress backward radiation caused by the eight coupling slots.

V. Antenna Prototype and Measured Result

The prototype of the proposed planar slot antenna array, shown in Fig. 7, is fabricated and measured to demonstrate the design strategy. The top and middle metallic layers are fabricated by using the traditional metal working process: The 72 slot regions, middle frame, and screw holes are manufactured using the line cutting technique. Fabrication of the bottom feed network layer is based on the traditional PCB technique. Twenty-four M2-type metallic screws and nuts are used to fix the three layers together tightly. Commercial SMA connector is soldered to the feed network for testing.

The reflection coefficient is measured using an N5247A vector network analyzer (10–67 GHz), and the gains and radiation patterns are measured using the NSI 2000 system.

The magnitude of the reflection coefficient is shown in Fig. 8(a). The simulated $|S_{11}|$ curve presents a single resonance characteristic, and the –10-dB impedance bandwidth is 5.3% from 19.49 to 20.53 GHz, while the measured curve has a double resonance characteristic with the bandwidth of 6.4% from 19.21 to 20.48 GHz. The difference comes from the different excitation approaches: In simulation, a lump port is created in a simple rectangular patch at the input of the power divider

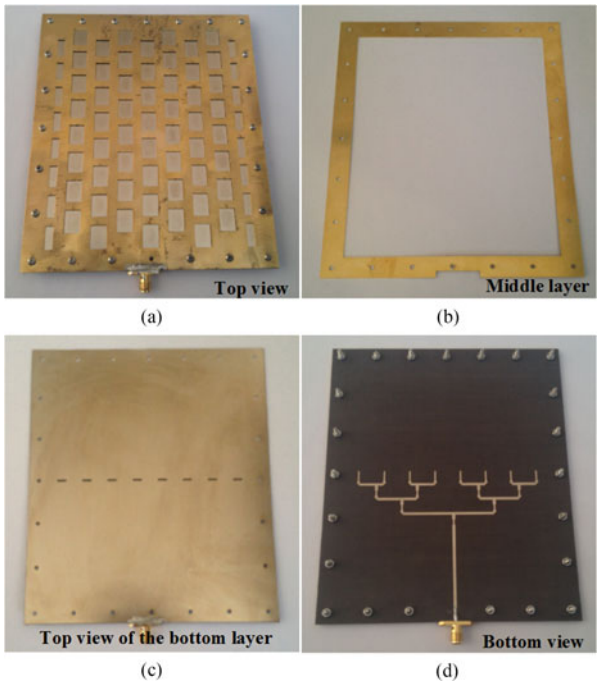

Fig. 7. Prototype of the proposed planar slot antenna array. (a) Top view of the whole antenna, (b) middle frame layer, (c) top view of the bottom layer, and (d) bottom view of the whole antenna.

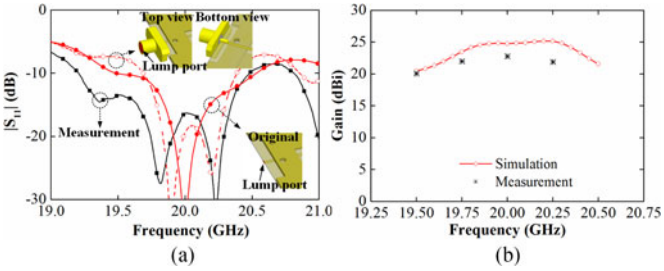

Fig. 8. (a) Measured and simulated magnitudes of reflection coefficients and (b) gains of the proposed planar slot antenna array.

as shown in the lower right inset, whereas an SMA connector is used in measurement. Based on the realistic prototype, the SMA connector is modeled in HFSS as shown in the upper middle inset. The simulated curve that is denoted as the dashed line with open circles agrees well with the measurement: It presents a double resonance characteristic as well. The reason is that the SMA connector causes the impedance loci on the Smith chart to rotate around the center. The measured gain is given in Fig. 8(b). The simulated gain ranges from 20.5 to 25.18 dBi, while the measured is from 20.05 to 22.75 dBi. An average gain drop of about 1.8 dB is mainly caused by the fact that the dielectric loss of substrate of the feeding network is higher than its nominal value.

The measured and simulated normalized radiation patterns in the two principal planes are plotted in Fig. 9. Here, the patterns within the elevation angle range of $\pm 60°$ are given. It is observed that the measured results agree well with the simulation. The beam directs to the broadside without any tilts attributing to the center-fed approach. The measured 3-dB beamwidths in the

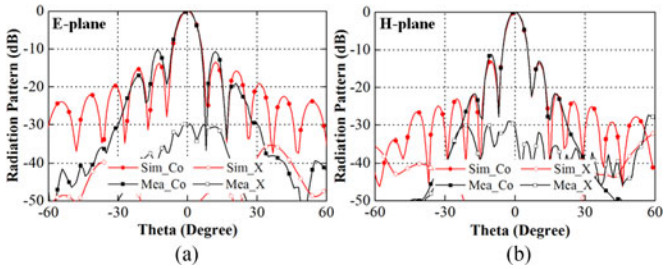

Fig. 9. Measured and simulated normalized radiation patterns in the two principal planes of the proposed planar slot antenna array at 20 GHz. (a) *E*-plane. (b) *H*-plane.

E- and *H*-plane are 7.5° and 6.3°, respectively, which are completely the same as the simulated results. The measured peak sidelobe levels are –10.21 and –11.26 dB, and the cross-polar levels are –29.73 and –27.38 dB in the *E*- and *H*-plane, respectively. Note that the measured sidelobe levels are far lower than the simulation when the elevation angles exceed 24° in both principal planes. This is because the finite near-field sampling area cannot comprise all the realistic near-field data in full space, and the far-field pattern is approximately calculated from the measured near-field sampling data using fast Fourier transformation.

VI. Conclusion

A new structure of air substrate planar slot antenna array based on ACCPW is proposed. By blocking eight coplanar ACCPWs alternatively every half-wavelength, and arranging the antenna layout in a mirrored way, a compact antenna structure and a large radiating aperture with synchronous fields are achieved. A line source fed in the array center is used to suppress beam tilt. The fabricated prototype shows a bandwidth of 6.4% and a peak gain of 22.75 dBi.

References

[1] I. Papapolymerou, R. F. Drayton, and L. P. B. Katehi, "Micromachined patch antennas," *IEEE Trans. Antennas Propag.*, vol. 46, no. 2, pp. 275–283, Feb. 1998.

[2] Y. She, J. Hirokawa, M. Ando, D. Hanatani, and M. Fujimoto, "LTCC partially-filled post-wall rectangular-waveguide slot array antenna in the millimeter-wave band," *IEICE Trans. Electron.*, vol. E95-C, no. 10, pp. 1635–1642, Oct. 2012.

[3] Y. She, R. Fujino, J. Hirokawa, M. Ando, D. Hanatani, and M. Fujimoto, "LTCC oversized rectangular waveguide slot array antenna with air-layer in the radiating part in the millimeter-wave band," *IEEE Trans. Antennas Propag.*, vol. 61, no. 4, pp. 1777–1783, Apr. 2013.

[4] Y. She, J. Hirokawa, M. Ando, D. Hanatani, and M. Fujimoto, "LTCC oversized rectangular waveguide slot array antenna with air-layer," *IEEE Trans. Antennas Propag.*, vol. 63, no. 2, pp. 5850–5854, Dec. 2015.

[5] L. Chang, Z. Zhang, Y. Li and Z. Feng, "All-metal antenna array based on microstrip line structure," *IEEE Trans. Antennas Propag.*, vol. 64, no. 1, pp. 351–355, Jan. 2016.

[6] L. Chang, Y. Li, Z. Zhang and Z. Feng, "A compact all-metallic cavity-cascaded antenna," *Electron. Lett.*, vol. 52, no. 6, pp. 413–414, Mar. 2016.

[7] L. Chang, Z. Zhang, Y. Li, and Z Feng, "Wideband triangular cavity cascaded antennas," *IEEE Trans. Antennas Propag.*, vol. 64, no. 7, pp. 2840–2847, Jul. 2016.

[8] R. Simons, *Coplanar Waveguide Circuits, Components, and Systems*, 2nd ed. New York, NY, USA: Wiley, 2004, pp. 107–108.